An Adaptive Control Framework for Underactuated Switched Euler–Lagrange Systems

Roy, Spandan; Baldi, Simone; Ioannou, Petros A.

DOI
10.1109/TAC.2021.3108507

Publication date
2022

Document Version
Final published version

Published in
IEEE Transactions on Automatic Control

An Adaptive Control Framework for Underactuated Switched Euler–Lagrange Systems

Spandan Roy, Simone Baldi, and Petros A. Ioannou

***Abstract*—The control of underactuated Euler–Lagrange systems with uncertain and switched parameters is an important problem whose solution has many applications. The problem is challenging as standard adaptive control techniques do not extend to this class of systems due to structural constraints that lead to parameterization difficulties. This note proposes an adaptive switched control framework that handles the uncertainty and switched dynamics without imposing structural constraints. A case study inspired by autonomous vessel operations is used to show the effectiveness of the proposed approach.**

***Index Terms*—Euler–Lagrange (EL) systems, robust adaptive control, switched systems, underactuated systems.**

I. Introduction

Underactuated Euler–Lagrange (EL) dynamics are used to represent a large class of real-world systems where the number of available control inputs is less than the degrees of freedom: examples span from aerial/ground/marine vehicles to robotic systems [1]–[4]. Often, changing operating conditions require a switching mechanism orchestrating different regimes (or modes) of the underactuated EL dynamics. For example, in the emerging field of autonomous offshore vessels [5], [6], a crane vessel is known to exhibit different dynamics during the various stages of a construction work, as per effect of mooring/free-hanging transitions (cf., the phases in Fig. 1). In addition to parametric changes in mass and inertia, such transitions make the crane vessel dynamics intrinsically change, e.g., the "mooring force," due to swing in the crane wires caused by ship motion, appears only in phase 2 (cf., Section IV-A). This and other examples from several fields highlight the relevance of controlling the different regimes in underactuated EL systems. Approaches involving adaptive and switching control tools have been proposed for several classes of uncertain switched systems [7]–[11]: the main idea is to activate a different adaptive control action synchronized with the active mode of the system. However, to the best of the authors' knowledge, the problem of adaptive control of underactuated switched EL systems remains open. In fact, although stability results have appeared for underactuated EL systems, such results rely on *ad hoc* structural constraints for the mass matrix and for the uncertainties (symmetry conditions[1] and constant bounds [3], [4], [12]–[16]), which can be restrictive and not valid in general. Note that, such approaches are nonadaptive, and cannot accommodate large parametric uncertainties and switched dynamics. A challenge arises since traditional adaptive control techniques do not easily extend to this class of systems as underactuation makes it difficult to find appropriate parameterizations [e.g., linear-in-the-parameter (LIP)] [17]–[19]. The LIP form used to develop adaptive laws for fully actuated EL systems [17], [19] is not directly applicable in the presence of underactuation [20], unless detailed structural knowledge of the system (not available in general) is used to separate the parametric uncertainties from the system states [21].

This note addresses the aforementioned challenges of adaptive control with underactuation by following.

1) Designing and analyzing a stable and robust adaptive scheme without imposing structural constraints nor requiring detailed structural knowledge of the EL dynamics.
2) Proving that the proposed scheme can handle switched dynamics, i.e., changing-regime scenarios.

The rest of this article is organized as follows: Section II describes the class of EL systems, Section III details the proposed control framework along with stability analysis, an autonomous vessel example is used in Section IV, and finally, Section V concludes this article.

The following notation is used throughout this article: $\lambda_{\max}(\bullet)$, $\lambda_{\min}(\bullet)$, and $||\bullet||$ represent maximum eigenvalue, minimum eigenvalue, and Euclidean norm of $(\bullet)$, respectively; $\mathbf{I}$ denotes identity matrix with appropriate dimension; and $\boldsymbol{\Xi} > \mathbf{0}$ denotes a positive definite matrix $\boldsymbol{\Xi}$.

II. System Dynamics and Problem Formulation

We consider n degrees-of-freedom switched underactuated EL dynamics in the following form:

$$\check{\mathbf{M}}_{\sigma(t)}(\bar{\mathbf{q}}(t))\ddot{\bar{\mathbf{q}}}(t) + \check{\mathbf{C}}_{\sigma(t)}(\bar{\mathbf{q}}(t), \dot{\bar{\mathbf{q}}}(t))\dot{\bar{\mathbf{q}}}(t) + \check{\mathbf{F}}_{\sigma(t)}(\bar{\mathbf{q}}(t), \dot{\bar{\mathbf{q}}}(t)) + \check{\mathbf{G}}_{\sigma(t)}(\bar{\mathbf{q}}(t))\bar{\mathbf{q}}(t) + \check{\mathbf{d}}_{\sigma(t)}(t) = \bar{\boldsymbol{\tau}}_{\sigma(t)}(t) \quad (1)$$

where $\bar{\mathbf{q}}$ and $\dot{\bar{\mathbf{q}}} \in \mathbb{R}^n$ are vectors of generalized positions and velocities assumed to be available for the measurement. For each mode indexed by σ, $\check{\mathbf{M}}_\sigma(\bar{\mathbf{q}}) = \check{\mathbf{M}}_\sigma^T(\bar{\mathbf{q}}) \in \mathbb{R}^{n\times n}$ is the mass/inertia matrix; $\check{\mathbf{C}}_\sigma(\bar{\mathbf{q}}, \dot{\bar{\mathbf{q}}})\dot{\bar{\mathbf{q}}} \in \mathbb{R}^n$ are the Coriolis, centripetal forces; $\check{\mathbf{F}}_\sigma(\bar{\mathbf{q}}, \dot{\bar{\mathbf{q}}}) \in \mathbb{R}^n$ are damping and friction forces; $\check{\mathbf{G}}_\sigma(\bar{\mathbf{q}})\bar{\mathbf{q}} \in \mathbb{R}^n$ are position-dependent

[1]The term "symmetry condition," coined in [3] indicates that the mass matrix depends on only the actuated states or only the nonactuated states. It is not to be confused with the fact that the mass matrix is symmetric.

Manuscript received 19 December 2019; revised 5 August 2020, 15 March 2021, and 24 June 2021; accepted 22 August 2021. Date of publication 30 August 2021; date of current version 29 July 2022. This work was supported in part by TU Delft grant "Autonomous Operation of Crane Vessels" (PLD-PLD004), in part by Double Innovation Plan (4207012004), in part by Special Funding for Overseas talents (6207011901), and in part by Natural Science Foundation of China under Grant 62073074. Recommended by Associate Editor G. Gu. *(Corresponding author: Simone Baldi.)*

Spandan Roy is with the Robotics Research Center, International Institute of Information Technology Hyderabad, Hyderabad 500032, India, and also with the Delft Center for Systems and Control, Delft University of Technology, 2628CN Delft, The Netherlands (e-mail: sroy002@gmail.com).

Simone Baldi is with the School of Mathematics, Southeast University, Nanjing 210096, China, and also with the Delft Center for Systems and Control, Delft University of Technology, 2628CD Delft, The Netherlands (e-mail: s.baldi@tudelft.nl).

Petros A. Ioannou is with the Department of Electrical Engineering, University of Southern California, Los Angeles, CA 90007 USA (e-mail: ioannou@usc.edu).

Color versions of one or more figures in this article are available at https://doi.org/10.1109/TAC.2021.3108507.

Digital Object Identifier 10.1109/TAC.2021.3108507

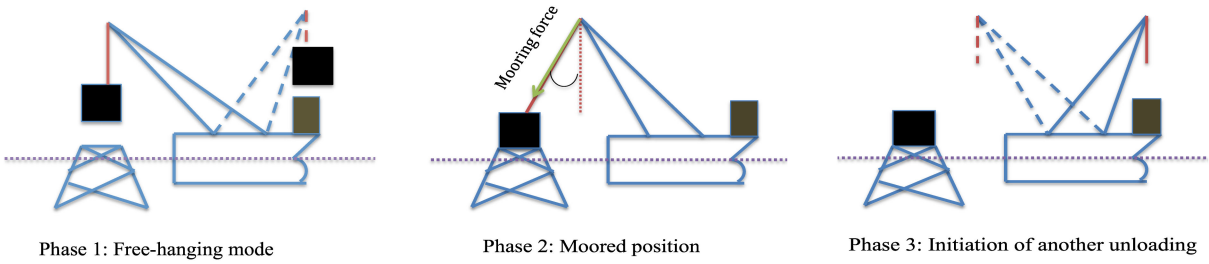

Fig. 1. Schematics of typical phases of operation for an offshore crane vessel system.

forces such as restoring forces; and $\check{\mathbf{d}}_\sigma \in \mathbb{R}^n$ are external disturbances. The control input $\bar{\boldsymbol{\tau}}_\sigma \in \mathbb{R}^n$ contains $(n-m)$ zero entries, where $m < n$ due to underactuation. The following class of systems is considered.

Assumption 1: The state and input dimensions satisfy $(n-m) \leq m < n$.

Remark 1 (Generality of the class): Assumption 1 implies that the number of actuated states is not fewer than the nonactuated states. Several underactuated EL systems of practical interest belong to such class (c.f., the examples in [1], [2], [4], [14]–[16], and [22]–[25]). Dynamics (1) excludes nonholonomic EL systems [26], which can be the subject of future research.

The signal $\sigma(\cdot)$: $[0\,\infty) \mapsto \Omega$ in (1) is a piecewise constant function of time, called the *switching signal*. It takes values in $\Omega = \{1, 2, \ldots, N\}$ and determines the active mode dynamics at time t (note that σ causes switches in the system functions but not in the states). The following class of switching signals is considered.

Definition 1 (Average dwell time (ADT) [27]): Let $N_\sigma(t_1, t_2)$ denote the number of discontinuities in the interval $[t_1, t_2)$, where $t_2 \geq t_1 \geq 0$. Then, $\sigma(\cdot)$ has an average dwell time ϑ if for a given scalar $N_0 > 0$

$$N_\sigma(t_1, t_2) \leq N_0 + (t_2 - t_1)/\vartheta \;\; \forall t_2 \geq t_1 \geq 0 \tag{2}$$

where N_0 is referred to as the chatter bound.

Remark 2 (Switching policy): The time-dependent switching policy $\sigma(\cdot)$ characterized by (2) exhibits finite number of mode transitions in a finite time interval. On short time intervals, the number of transitions is upper bounded by N_0; and on long time intervals, the average number of transitions $N_\sigma(t_1, t_2)/(t_2 - t_1)$ is upper bounded by $1/\vartheta$ [27].

For convenience of notation, the states and dynamic terms in (1) are rewritten by distinguishing between the actuated and nonactuated subsystems as

$$\mathbf{M}_\sigma(\mathbf{q})\ddot{\mathbf{q}} + \mathbf{E}_\sigma(\mathbf{q}, \dot{\mathbf{q}}) + \mathbf{d}_\sigma = [\boldsymbol{\tau}_\sigma^T \; \mathbf{0}^T]^T \tag{3}$$

where $\mathbf{q} = [\mathbf{q_a}^T \; \mathbf{q_u}^T]^T, \mathbf{q_a} \in \mathbb{R}^m, \mathbf{q_u} \in \mathbb{R}^{(n-m)}$

$$\mathbf{M}_\sigma \triangleq \begin{bmatrix} \mathbf{M_{aa\sigma}} & \mathbf{M_{au\sigma}} \\ \mathbf{M}_{\mathbf{au}\sigma}^T & \mathbf{M_{uu\sigma}} \end{bmatrix} \tag{4}$$

$$\mathbf{E}_\sigma \triangleq \mathbf{C}_\sigma(\mathbf{q}, \dot{\mathbf{q}})\dot{\mathbf{q}} + \mathbf{G}_\sigma(\mathbf{q})\mathbf{q} + \mathbf{F}_\sigma(\mathbf{q}, \dot{\mathbf{q}}) = \begin{bmatrix} \mathbf{E}_{\mathbf{a}\sigma}^T & \mathbf{E}_{\mathbf{u}\sigma}^T \end{bmatrix}^T \tag{5}$$

$\mathbf{E_{a\sigma}} \in \mathbb{R}^m, \mathbf{E_{u\sigma}} \in \mathbb{R}^{(n-m)}$

$$\mathbf{d}_\sigma \triangleq \begin{bmatrix} \mathbf{d}_{\mathbf{a}\sigma}^T & \mathbf{d}_{\mathbf{u}\sigma}^T \end{bmatrix}^T, \mathbf{d_{a\sigma}} \in \mathbb{R}^m, \mathbf{d_{u\sigma}} \in \mathbb{R}^{(n-m)} \tag{6}$$

where $\mathbf{M}_\sigma, \mathbf{C}_\sigma, \mathbf{F}_\sigma, \mathbf{G}_\sigma$, and $\mathbf{d}_\sigma$ are obtained from $\check{\mathbf{M}}_\sigma, \check{\mathbf{C}}_\sigma, \check{\mathbf{F}}_\sigma, \check{\mathbf{G}}_\sigma$, and $\check{\mathbf{d}}_\sigma$, respectively, by arranging the actuated $(\mathbf{q_a})$ and nonactuated $(\mathbf{q_u})$ states. Note that the disturbance affects both the actuated and nonactuated subsystem.

For most EL systems of practical interest, the following properties hold for each mode in (1) (cf., [1, ch. 6]).

Property 1: $\exists \overline{c}_\sigma, \overline{g}_\sigma, \overline{f}_\sigma, \overline{d}_\sigma \in \mathbb{R}^+$ such that $||\mathbf{C}_\sigma(\mathbf{q}, \dot{\mathbf{q}})|| \leq \overline{c}_\sigma||\dot{\mathbf{q}}||$, $||\mathbf{G}_\sigma(\mathbf{q})|| \leq \overline{g}_\sigma$, $||\mathbf{F}_\sigma(\mathbf{q}, \dot{\mathbf{q}})|| \leq \overline{f}_\sigma||\dot{\mathbf{q}}||$, and $||\mathbf{d}_\sigma(t)|| \leq \overline{d}_\sigma$.

Property 2: The matrix $\mathbf{M}_\sigma(\mathbf{q}) = \mathbf{M}_\sigma^T(\mathbf{q})$ is uniformly positive definite in the sense that $\exists \underline{m}_\sigma, \overline{m}_\sigma \in \mathbb{R}^+$ such that

$$0 < \underline{m}_\sigma \mathbf{I} \leq \mathbf{M}_\sigma^T(\mathbf{q}) \leq \overline{m}_\sigma \mathbf{I} \;\; \forall \mathbf{q}. \tag{7}$$

Assumption 2 (Parametric uncertainty): Consider the mass matrix decomposition as $\mathbf{M}_\sigma = \hat{\mathbf{M}}_\sigma + \Delta\mathbf{M}_\sigma$, where $\hat{\mathbf{M}}_\sigma$ and $\Delta\mathbf{M}_\sigma$ represent the nominal and uncertain part, respectively. $\hat{\mathbf{M}}_\sigma$ and an upper bound for $\Delta\mathbf{M}_\sigma$ are assumed to be known, whereas the terms $\mathbf{C}_\sigma, \mathbf{F}_\sigma, \mathbf{G}_\sigma$, and $\mathbf{d}_\sigma$ and their upper bounds $\overline{c}_\sigma, \overline{g}_\sigma, \overline{f}_\sigma$, and $\overline{d}_\sigma$ are considered to be unknown.

Assumption 2 defines the uncertainty assumed in this article and is further discussed at the end of the section. The dynamics (3) can be rearranged as

$$\ddot{\mathbf{q}}_\mathbf{u} = -\mathbf{M}_{\mathbf{uu}\sigma}^{-1}\mathbf{M}_{\mathbf{au}\sigma}\ddot{\mathbf{q}}_\mathbf{a} + \mathbf{h}_{\mathbf{u}\sigma} \tag{8a}$$

$$\ddot{\mathbf{q}}_\mathbf{a} = \mathbf{M}_{\mathbf{s}\sigma}^{-1}\boldsymbol{\tau}_\sigma + \mathbf{h}_{\mathbf{a}\sigma} \tag{8b}$$

where $\mathbf{h}_{\mathbf{u}\sigma} \triangleq \mathbf{M}_{\mathbf{uu}\sigma}^{-1}(\mathbf{E}_{\mathbf{u}\sigma} + \mathbf{d}_{\mathbf{u}\sigma})$

$$\mathbf{h}_{\mathbf{a}\sigma} \triangleq \mathbf{M}_{\mathbf{s}\sigma}^{-1}(\mathbf{E}_{\mathbf{a}\sigma} + \mathbf{d}_{\mathbf{a}\sigma} - \mathbf{M}_{\mathbf{au}}\mathbf{M}_{\mathbf{uu}\sigma}^{-1}(\mathbf{E}_{\mathbf{u}\sigma} + \mathbf{d}_{\mathbf{u}\sigma}))$$

$$\mathbf{M}_{\mathbf{s}\sigma} \triangleq \mathbf{M}_{\mathbf{aa}\sigma} - \mathbf{M}_{\mathbf{au}\sigma}\mathbf{M}_{\mathbf{uu}\sigma}^{-1}\mathbf{M}_{\mathbf{au}\sigma}^T.$$

As $\mathbf{M}_\sigma > \mathbf{0}$ by *Property 2*, the existence of $\mathbf{M}_{\mathbf{s}\sigma}^{-1}, \mathbf{M}_{\mathbf{aa}\sigma}^{-1}$, and $\mathbf{M}_{\mathbf{uu}\sigma}^{-1}$ is always guaranteed [24], [28]. The following requirement is a well-known condition for the controllability of underactuated EL systems (see[20] and [29]).

Assumption 3: The block $\mathbf{M_{au}}(\mathbf{q})$ is full rank $\forall \mathbf{q} \in \mathbb{R}^n$.

We should note that no structural constraints are imposed on (1), such as the *symmetry condition* of the mass matrix $\mathbf{M}_\sigma(\mathbf{q}) = \mathbf{M}_\sigma(\mathbf{q_a})$ or $\mathbf{M}_\sigma(\mathbf{q}) = \mathbf{M}_\sigma(\mathbf{q_u})$ [2]–[4], [12], [13] or *a priori* boundedness of state derivatives/ nonactuated states [2], [14]–[16]. We only require an upper bound on the mass matrix uncertainty [cf., (13)], which can be obtained without structural knowledge of the dynamics based on the maximum payload of the system to be controlled [30], [31].

Control Objective: Under Properties 1 and 2, Definition 1, and Assumptions 1–3, design a stable switched adaptive control mechanism for the system (8) to track a desired trajectory $\mathbf{q}^d(t) \triangleq [\mathbf{q_a^d}^T \; \mathbf{q_u^d}^T]^T$, where it is assumed that $\mathbf{q}^d, \dot{\mathbf{q}}^d, \ddot{\mathbf{q}}^d \in \mathcal{L}_\infty$.

In the following section, we present the design and analysis of a control scheme that meets the aforementioned control objective.

III. Controller Design and Analysis

Let $\mathbf{e_a}(t) \triangleq \mathbf{q_a}(t) - \mathbf{q_a^d}(t)$ be the tracking error of the actuated states and $\mathbf{e_u}(t) \triangleq \mathbf{q_u}(t) - \mathbf{q_u^d}(t)$ be the tracking error of the non-actuated ones. Define

$$\mathbf{r} \triangleq \boldsymbol{\Upsilon}_\mathbf{a}\dot{\mathbf{e}}_\mathbf{a} + \boldsymbol{\Gamma}_\mathbf{a}\mathbf{e_a} + \boldsymbol{\Upsilon}_\mathbf{u}\dot{\mathbf{e}}_\mathbf{u} + \boldsymbol{\Gamma}_\mathbf{u}\mathbf{e_u} \tag{9}$$

with user-defined gain matrices $\boldsymbol{\Upsilon}_\mathbf{a}, \boldsymbol{\Gamma}_\mathbf{a} \in \mathbb{R}^{m\times m}$ and $\boldsymbol{\Upsilon}_\mathbf{u}, \boldsymbol{\Gamma}_\mathbf{u} \in \mathbb{R}^{m\times(n-m)}$ satisfying

$$\boldsymbol{\Upsilon}_\mathbf{a} > \mathbf{0}, \boldsymbol{\Gamma}_\mathbf{a} > \mathbf{0}, \boldsymbol{\Upsilon}_\mathbf{a}^{-1}\boldsymbol{\Gamma}_\mathbf{a} > \mathbf{0} \tag{10a}$$

$$\boldsymbol{\Upsilon}_\mathbf{u}, \boldsymbol{\Gamma}_\mathbf{u} \text{ are of full rank } (n-m). \tag{10b}$$

Using (8a) and (8b), we obtain the time derivative of (9)

$$\begin{aligned}\dot{\mathbf{r}} &= (\boldsymbol{\Upsilon}_\mathbf{a} - \boldsymbol{\Upsilon}_\mathbf{u}\mathbf{M}_{\mathbf{uu}\sigma}^{-1}\mathbf{M}_{\mathbf{au}\sigma})(\mathbf{M}_{\mathbf{s}\sigma}^{-1}\boldsymbol{\tau} + \mathbf{h}_{\mathbf{a}\sigma}) + \boldsymbol{\Upsilon}_\mathbf{u}\mathbf{h}_{\mathbf{u}\sigma} \\ &\quad + \boldsymbol{\Gamma}_\mathbf{a}\dot{\mathbf{e}}_\mathbf{a} + \boldsymbol{\Gamma}_\mathbf{u}\dot{\mathbf{e}}_\mathbf{u} - \boldsymbol{\Upsilon}_\mathbf{a}\ddot{\mathbf{q}}_\mathbf{a}^d - \boldsymbol{\Upsilon}_\mathbf{u}\ddot{\mathbf{q}}_\mathbf{u}^d \\ &= \mathbf{b}_\sigma\boldsymbol{\tau}_\sigma + \boldsymbol{\phi}_\sigma + \mathbf{S}_r \end{aligned} \tag{11}$$

with

$$\begin{aligned}\mathbf{b}_\sigma &\triangleq (\boldsymbol{\Upsilon}_\mathbf{a} - \boldsymbol{\Upsilon}_\mathbf{u}\mathbf{M}_{\mathbf{uu}\sigma}^{-1}\mathbf{M}_{\mathbf{au}\sigma})\mathbf{M}_{\mathbf{s}\sigma}^{-1} \\ \boldsymbol{\phi}_\sigma &\triangleq (\boldsymbol{\Upsilon}_\mathbf{a} - \boldsymbol{\Upsilon}_\mathbf{u}\mathbf{M}_{\mathbf{uu}\sigma}^{-1}\mathbf{M}_{\mathbf{au}\sigma})\mathbf{h}_{\mathbf{a}\sigma} + \boldsymbol{\Upsilon}_\mathbf{u}\mathbf{h}_{\mathbf{u}\sigma} \\ \mathbf{S}_r &\triangleq \boldsymbol{\Gamma}_\mathbf{a}\dot{\mathbf{e}}_\mathbf{a} + \boldsymbol{\Gamma}_\mathbf{u}\dot{\mathbf{e}}_\mathbf{u} - \boldsymbol{\Upsilon}_\mathbf{a}\ddot{\mathbf{q}}_\mathbf{a}^d - \boldsymbol{\Upsilon}_\mathbf{u}\ddot{\mathbf{q}}_\mathbf{u}^d.\end{aligned}$$

We are now in the position to design the control law as

$$\boldsymbol{\tau}_\sigma = \hat{\mathbf{b}}_\sigma^{-1}(-\boldsymbol{\Lambda}_\sigma\mathbf{r} - \mathbf{S}_r - \Delta\boldsymbol{\tau}_\sigma) \tag{12a}$$

$$\Delta\boldsymbol{\tau}_\sigma = \varpi_\sigma \frac{\mathbf{r}}{\sqrt{||\mathbf{r}||^2 + \epsilon}} \tag{12b}$$

where $\boldsymbol{\Lambda}_\sigma > \mathbf{0}$ is a user-defined gain matrix; and $\Delta\boldsymbol{\tau}_\sigma$ tackles the following uncertainties: ϖ_σ is a design parameter to be selected and $\epsilon > 0$ is a small scalar to avoid chattering. Finally, $\hat{\mathbf{b}}_\sigma$, the nominal value of $\mathbf{b}_\sigma$ is designed such that

$$||\mathbf{b}_\sigma\hat{\mathbf{b}}_\sigma^{-1} - \mathbf{I}|| \le \alpha < 1 \ \ \forall\sigma \in \Omega \tag{13}$$

where α is a known scalar available for the control design.

Remark 3 (Mass matrix uncertainty): The condition of $\alpha < 1$ in (13) implies that the uncertainty in $\mathbf{b}_\sigma$ (and consequently, in the mass matrix) cannot be arbitrarily large in line with Assumption 2.

We want now to find a suitable description for the uncertainty of $\mathbf{E}_\sigma$ in (3) *without its structural knowledge*, that will allow us to design an appropriate term ϖ_σ in (12b). Substituting (12b) into (11), we obtain

$$\begin{aligned}\dot{\mathbf{r}} &= -\boldsymbol{\Lambda}_\sigma\mathbf{r} - \Delta\boldsymbol{\tau}_\sigma + \boldsymbol{\Psi}_\sigma - (\mathbf{b}_\sigma\hat{\mathbf{b}}_\sigma^{-1} - \mathbf{I})\Delta\boldsymbol{\tau}_\sigma \\ \text{with} \boldsymbol{\Psi}_\sigma &\triangleq \boldsymbol{\phi}_\sigma - (\mathbf{b}_\sigma\hat{\mathbf{b}}_\sigma^{-1} - \mathbf{I})(\boldsymbol{\Lambda}_\sigma\mathbf{r} + \mathbf{S}_r).\end{aligned} \tag{14}$$

Using *Properties 1* and *2* and taking $\boldsymbol{\chi} \triangleq [\mathbf{q}^T \ \dot{\mathbf{q}}^T]^T$, one can verify (cf., [1]) the existence of $\theta_i \in \mathbb{R}^+, i = 0, 1, 2$ such that

$$||\mathbf{E}_\sigma(\boldsymbol{\chi})|| \le \theta_{0\sigma} + \theta_{1\sigma}||\boldsymbol{\chi}|| + \theta_{2\sigma}||\boldsymbol{\chi}||^2. \tag{15}$$

Let $\boldsymbol{\xi} \triangleq [\mathbf{e_a}^T \ \mathbf{e_u}^T \ \dot{\mathbf{e}}_\mathbf{a}^T \ \dot{\mathbf{e}}_\mathbf{u}^T]^T$. Then, utilizing the boundedness conditions $\mathbf{q}^d, \dot{\mathbf{q}}^d, \ddot{\mathbf{q}}^d \in \mathcal{L}_\infty$ and (15), one has

$$||\boldsymbol{\Psi}_\sigma|| \le \theta_{0\sigma}^* + \theta_{1\sigma}^*||\boldsymbol{\xi}|| + \theta_{2\sigma}^*||\boldsymbol{\xi}||^2 \tag{16}$$

where $\theta_{i\sigma}^*, i = 0, 1, 2$ are positive scalars that according to Assumption 2 are *unknown*. Using (8a) and (8b), the dynamics of $\mathbf{e_u}$ is written as

$$\begin{aligned}\ddot{\mathbf{e}}_\mathbf{u} &= \ddot{\mathbf{q}}_\mathbf{u} - \ddot{\mathbf{q}}_\mathbf{u}^d = -\mathbf{M}_{\mathbf{uu}\sigma}^{-1}\mathbf{M}_{\mathbf{au}\sigma}\ddot{\mathbf{q}}_\mathbf{a} + \mathbf{h}_{\mathbf{u}\sigma} - \ddot{\mathbf{q}}_\mathbf{u}^d \\ &= -\mathbf{M}_{\mathbf{uu}\sigma}^{-1}\mathbf{M}_{\mathbf{au}\sigma}(\mathbf{M}_{\mathbf{s}\sigma}^{-1}\boldsymbol{\tau}_\sigma + \mathbf{h}_{\mathbf{a}\sigma}) + \mathbf{h}_{\mathbf{u}\sigma} - \ddot{\mathbf{q}}_\mathbf{u}^d.\end{aligned} \tag{17}$$

Substituting (12b) into (17) gives

$$\begin{aligned}\ddot{\mathbf{e}}_\mathbf{u} &= \mathbf{g}_\sigma(\boldsymbol{\Lambda}_\sigma\mathbf{r} + \mathbf{S}_r + \Delta\boldsymbol{\tau}_\sigma) - \overline{\boldsymbol{\phi}}_\sigma \\ \text{with} \ \overline{\boldsymbol{\phi}}_\sigma &\triangleq (\mathbf{M}_{\mathbf{uu}\sigma}^{-1}\mathbf{M}_{\mathbf{au}\sigma}\mathbf{h}_{\mathbf{a}\sigma} + \mathbf{h}_{\mathbf{u}\sigma} - \ddot{\mathbf{q}}_\mathbf{u}^d) \\ \mathbf{g}_\sigma &\triangleq (\mathbf{M}_{\mathbf{uu}\sigma}^{-1}\mathbf{M}_{\mathbf{au}\sigma}\mathbf{M}_{\mathbf{s}\sigma}^{-1})\hat{\mathbf{b}}_\sigma^{-1}.\end{aligned} \tag{18}$$

Assumption 1 allows us to design a constant full rank matrix $\mathbf{H}_\sigma \in \mathbb{R}^{(n-m)\times m}$ such that the following holds:

$$\mathbf{K}_{1\sigma} \triangleq \mathbf{H}_\sigma\boldsymbol{\Lambda}_\sigma\boldsymbol{\Gamma}_\mathbf{u} > \mathbf{0}, \ \mathbf{K}_{2\sigma} \triangleq \mathbf{H}_\sigma\boldsymbol{\Lambda}_\sigma\boldsymbol{\Upsilon}_\mathbf{u} > \mathbf{0}. \tag{19}$$

Adding and subtracting $\mathbf{H}_\sigma\boldsymbol{\Lambda}_\sigma\mathbf{r}$ in (18) and defining $\mathbf{x} \triangleq [\mathbf{e_u}^T \ \dot{\mathbf{e}}_\mathbf{u}^T]^T$, $\mathbf{B} \triangleq \begin{bmatrix}\mathbf{0} & \mathbf{I}\end{bmatrix}^T$, and the Hurwitz matrix $\mathbf{A}_\sigma \triangleq \begin{bmatrix}\mathbf{0} & \mathbf{I} \\ -\mathbf{K}_{1\sigma} & -\mathbf{K}_{2\sigma}\end{bmatrix}$ gives

$$\dot{\mathbf{x}} = \mathbf{A}_\sigma\mathbf{x} + \mathbf{B}(\mathbf{g}_\sigma\Delta\boldsymbol{\tau}_\sigma + \overline{\overline{\boldsymbol{\phi}}}_\sigma) \tag{20}$$

where $\overline{\overline{\boldsymbol{\phi}}}_\sigma \triangleq \mathbf{g}_\sigma\mathbf{S}_r + (\mathbf{H}_\sigma + \mathbf{g}_\sigma)\boldsymbol{\Lambda}_\sigma\mathbf{r} - \overline{\boldsymbol{\phi}}_\sigma - \mathbf{H}_\sigma\boldsymbol{\Lambda}_\sigma(\boldsymbol{\Upsilon}_\mathbf{a}\dot{\mathbf{e}}_\mathbf{a} + \boldsymbol{\Gamma}_\mathbf{a}\mathbf{e_a})$. Again, using *Properties 1 and 2* and the design condition $\mathbf{q}^d, \dot{\mathbf{q}}^d, \ddot{\mathbf{q}}^d \in \mathcal{L}_\infty$, the following upper bound is obtained:

$$||\overline{\overline{\boldsymbol{\phi}}}_\sigma||||\mathbf{P}_\sigma\mathbf{B}|| \le \left(\theta_{0\sigma}^{**} + \theta_{1\sigma}^{**}||\boldsymbol{\xi}|| + \theta_{2\sigma}^{**}||\boldsymbol{\xi}||^2\right) \tag{21}$$

where $\theta_{i\sigma}^{**} \in \mathbb{R}^+, i = 0, 1, 2$ are unknown scalars; and $\mathbf{P}_\sigma > \mathbf{0}$ is the solution of the Lyapunov equation $\mathbf{A}_\sigma^T\mathbf{P}_\sigma + \mathbf{P}_\sigma\mathbf{A}_\sigma = -\mathbf{Q}_\sigma$ for some $\mathbf{Q}_\sigma > \mathbf{0}$.

Remark 4 (LIP upper bounds): The inequalities (16) and (21) show that the upper bounds for $||\boldsymbol{\Psi}_\sigma||$ and $||\overline{\overline{\boldsymbol{\phi}}}_\sigma||$ are linear with respect to the unknown parameters, a property that is crucial in designing parameter estimators for these parameters.

The structures of the upper bounds of $||\boldsymbol{\Psi}_\sigma||$ and $||\overline{\overline{\boldsymbol{\phi}}}_\sigma||$ in (16) and (21) suggest the following design of ϖ_σ in (12b):

$$\varpi_\sigma = \frac{\varphi}{(1-\alpha)}(\hat{\theta}_{0\sigma} + \hat{\theta}_{1\sigma}||\boldsymbol{\xi}|| + \hat{\theta}_{2\sigma}||\boldsymbol{\xi}||^2 + \eta_\sigma + \gamma_\sigma) \tag{22}$$

where $\hat{\theta}_{ip}$ is the estimate of $\bar{\theta}_{ip}^* \triangleq \max\{\theta_{ip}^*, \theta_{ip}^{**}\}, i = 0, 1, 2$ at time t to be generated by an adaptive law; $\varphi > 1$ is a user-defined scalar; and η_p and γ_p are to be designed for the closed-loop system stability. Let us now denote with $p \in \Omega$ an active mode and with $\overline{p} \in \Omega$ an inactive one, then, the following adaptive laws are proposed for $(\hat{\theta}_{ip}, \eta_p, \gamma_p)$ and $(\hat{\theta}_{i\overline{p}}, \eta_{\overline{p}}, \gamma_{\overline{p}})$:

$$\dot{\hat{\theta}}_{ip} = (||\mathbf{r}|| + ||\mathbf{x}||)||\boldsymbol{\xi}||^i - \zeta_{ip}\hat{\theta}_{ip}\beta_p||\mathbf{x}||||\boldsymbol{\xi}||^i, \ \dot{\gamma}_p = 0 \tag{23a}$$

$$\begin{aligned}\dot{\eta}_p = -\eta_p &\left\{\delta_{0p} + \delta_{1p}(||\boldsymbol{\xi}||^5 - ||\boldsymbol{\xi}||^4) + \delta_{2p}||\mathbf{x}||\right\} \\ &+ (||\mathbf{r}|| + ||\mathbf{x}||) + \delta_{0p}\nu_p\end{aligned} \tag{23b}$$

$$\dot{\hat{\theta}}_{i\overline{p}} = 0, \ \dot{\gamma}_{\overline{p}} = -\left(\overline{\varsigma}_{\overline{p}} + \frac{\varrho_{\overline{p}}}{2}\left(\sum_{i=0}^{2}\hat{\theta}_{i\overline{p}}^2 + \eta_{\overline{p}}^2\right)\right)\gamma_{\overline{p}} + \overline{\varsigma}_{\overline{p}}\overline{\nu}_{\overline{p}}$$

$$\dot{\eta}_{\overline{p}} = 0 \tag{23c}$$

$$\text{and} \ \ \delta_{0p} \ge \delta_{1p} + \varrho_p/2, \ \overline{\varsigma}_{\overline{p}} \ge \varrho_{\overline{p}}/2 \tag{23d}$$

$$\beta_p > 1 + (\varphi\overline{\alpha}/(1-\alpha)), \ ||\mathbf{P}_p\mathbf{B}\mathbf{g}_p|| \le \overline{\alpha} \ \forall p \in \Omega \tag{23e}$$

$$\hat{\theta}_{ip}(t_0) > 0, \ \eta_p(t_0) > \nu_{1p}, \ \gamma_{\overline{p}}(t_0) > \overline{\nu}_{\overline{p}} \tag{23f}$$

where t_0 is the initial time, $\delta_{ip}, \zeta_{ip}, \beta_p, \overline{\varsigma}_{\overline{p}}, \nu_p, \overline{\nu}_{\overline{p}} \in \mathbb{R}^+, i = 0, 1, 2$ are static design scalars, and

$$\varrho_\sigma \triangleq \frac{\min\{\lambda_{\min}(\boldsymbol{\Lambda}_\sigma), \ (1/2)\lambda_{\min}(\mathbf{Q}_\sigma)\}}{\max\{(1/2), \ (1/2)\lambda_{\max}(\mathbf{P}_\sigma)\}} > 0. \tag{24}$$

Let us define $\kappa_M \triangleq \max_{p\in\Omega} \lambda_{\max}(\mathbf{P}_p)$ and $\kappa_m \triangleq \min_{p\in\Omega} \lambda_{\min}(\mathbf{P}_p)$. Following Definition 1, let us consider the switching signal $\sigma(\cdot)$ with an average dwell time ϑ satisfying

$$\vartheta > \ln \mu/\varrho \tag{25}$$

where $\mu \triangleq \kappa_M/\kappa_m$ and $\varrho \triangleq \min_{p\in\Omega}\{\varrho_p\}$.

Remark 5 (Codesign of switching and control law): The relation (25) highlights that switching and control laws are interconnected via the design parameters ($\mathbf{\Lambda}_\sigma, \mathbf{P}_\sigma,$ and $\mathbf{Q}_\sigma$) having the following codesign steps: based on the expected duration of the operational phases and expected number of mode transitions in a finite time interval according to the ADT inequality (2), one can determine the desirable ADT ϑ; then, $(\mathbf{\Lambda}_\sigma, \mathbf{P}_\sigma, \mathbf{Q}_\sigma)$ can be designed to yield $\vartheta > \ln \mu/\varrho$ as per (25).

The stability and robustness properties of the closed-loop system (8) are given by the following Theorem.

Theorem 1: Under Assumptions 1–3, Definition 1 and Properties 1 and 2, the closed-loop trajectories of (8) employing the control laws (12) and (22) with adaptive law (23) and (24), switching law (25) and gain designs (10), (13), and (19) are uniformly bounded. Furthermore, the tracking errors converge to a residual set whose size depends on unmodeled dynamics/switching and can be tuned via the design parameters (cf., (46), (50), and (52) in Appendix).

Proof: See Appendix. ■

Remark 6 (Robust adaptation): The analysis in the appendix covers robustness of the proposed adaptive scheme in the presence of unmodeled terms affecting (16) and (21), since no knowledge of the uncertainty bounds is required in these terms. Recall that, even for LTI uncertain systems, the lack of knowledge of the uncertainty bounds prevents in general asymptotic tracking in robust adaptive control [17, Sec. 8.4.1].

IV. Case Study

A scenario as in Fig. 1 can be described by an underactuated six degrees-of-freedom EL dynamics consisting of three modes (indexed by $\sigma = 1, 2, 3$ for each phase) [32], [33]

$$\dot{\bar{\mathbf{q}}} = \mathbf{J}(\bar{\mathbf{q}})\mathbf{v} \tag{26a}$$

$$\bar{\mathbf{M}}_\sigma \dot{\mathbf{v}} + \bar{\mathbf{F}}_\sigma \mathbf{v} + \bar{\mathbf{G}}_\sigma \bar{\mathbf{q}} + \mathbf{J}^{-T}(\bar{\mathbf{q}})\mathbf{d}_\sigma = \mathbf{u}_\sigma \tag{26b}$$

$$\text{where } \mathbf{J}(\bar{\mathbf{q}}) = \begin{bmatrix} \mathbf{R}_1(\bar{\mathbf{q}}) & \mathbf{0} \\ \mathbf{0} & \mathbf{R}_2(\bar{\mathbf{q}}) \end{bmatrix}, \mathbf{R}_2 = \begin{bmatrix} 1 & s_{\phi_r} t_\upsilon & c_{\phi_r} t_\upsilon \\ 0 & c_{\phi_r} & -s_{\phi_r} \\ 0 & s_{\phi_r}/c_\upsilon & c_{\phi_r}/c_\upsilon \end{bmatrix}$$

$$\mathbf{R}_1 = \begin{bmatrix} c_\psi c_\upsilon & -s_\psi c_{\phi_r} + c_\psi c_\upsilon s_{\phi_r} & s_\psi s_{\phi_r} + c_\psi c_\upsilon c_{\phi_r} \\ s_\psi c_\upsilon & c_\psi c_{\phi_r} + s_\psi c_\upsilon s_{\phi_r} & -c_\psi s_{\phi_r} + s_\psi c_\upsilon s_{\phi_r} \\ -c_\upsilon & c_\upsilon s_{\phi_r} & c_\upsilon c_{\phi_r} \end{bmatrix}$$

With $c_{(\cdot)} = \cos(\cdot)$; $s_{(\cdot)} = \sin(\cdot)$; $t_{(\cdot)} = \tan(\cdot)$; $\mathbf{v} = [v_x, v_y, v_z, v_{\phi_r}, v_\upsilon, v_\psi]^T$ contains the vessel velocity/angular velocity in body-fixed frame; $\bar{\mathbf{q}} = [x, y, z, \phi_r, \upsilon, \psi]^T$ comprises of north/east/down positions and roll/pitch/heading angles in Earth-fixed frame; $\bar{\mathbf{M}}_\sigma \in \mathbb{R}^{6\times 6}$ is the positive definite mass/inertia matrix; $\bar{\mathbf{F}}_\sigma \in \mathbb{R}^{6\times 6}$ combines the hydrodynamic damping and Coriolis matrices for simplicity; $\bar{\mathbf{G}}_\sigma = \bar{\mathbf{G}}^r_\sigma + \bar{\mathbf{G}}^m_\sigma \in \mathbb{R}^{6\times 6}$ is the combination of restoring ($\bar{\mathbf{G}}^r_\sigma$) and mooring ($\bar{\mathbf{G}}^m_\sigma$) matrices; $\mathbf{u}_\sigma = [u_{x_\sigma}\ u_{y_\sigma}\ 0\ 0\ 0\ u_{\psi_\sigma}]^T$ contains the three available control inputs; and $\mathbf{d}_\sigma$ combines the external effects of wave, sea current, and wind. Following the modeling approach in [32, Sec. 7.5], the dynamics in the Earth-fixed frame turns out to be

$$\check{\mathbf{M}}_\sigma(\bar{\mathbf{q}})\ddot{\bar{\mathbf{q}}} + \check{\mathbf{E}}_\sigma(\bar{\mathbf{q}}, \dot{\bar{\mathbf{q}}}) + \check{\mathbf{d}}_\sigma = \bar{\boldsymbol{\tau}}_\sigma$$

where $\check{\mathbf{M}}_\sigma \triangleq \mathbf{J}^{-T}\bar{\mathbf{M}}_\sigma\mathbf{J}^{-1}$

$$\check{\mathbf{E}}_\sigma(\bar{\mathbf{q}}, \dot{\bar{\mathbf{q}}}) \triangleq (\mathbf{J}^{-T}\bar{\mathbf{F}}_\sigma\mathbf{J}^{-1} - \mathbf{J}^{-T}\bar{\mathbf{M}}_\sigma\mathbf{J}^{-1}\dot{\mathbf{J}}\mathbf{J}^{-1})\dot{\bar{\mathbf{q}}} + \mathbf{J}^{-T}\bar{\mathbf{G}}_\sigma$$

$$\bar{\boldsymbol{\tau}}_\sigma \triangleq \mathbf{J}^{-T}\mathbf{u}_\sigma = [\tau_{x_\sigma}\ \tau_{y_\sigma}\ 0\ 0\ 0\ \tau_{\psi_\sigma}]^T. \tag{27}$$

Note that $\check{\mathbf{M}}_\sigma$ depends on both actuated (ψ) and nonactuated states (ϕ_r, υ), thereby providing a challenging test case to verify the proposed framework.

A. Operating Regimes

It can be noted from Fig. 1 that not only $\bar{\mathbf{M}}_\sigma$ changes when switching from $\sigma = 2$ to $\sigma = 3$, but also that the mooring force $\bar{\mathbf{G}}^m_\sigma\mathbf{q}$ is active when $\sigma = 2$, while disappearing when $\sigma = 1, 3$. Using scaled system parameters as in [33], the changing regimes for the three phases are described by

$$\bar{\mathbf{F}}_1 = \bar{\mathbf{F}}_2 = \bar{\mathbf{F}}_3$$

$$= \begin{bmatrix} 0.09 & 0 & 0.01 & 0 & 0 & -0.03 \\ 0 & 0.08 & 0.015 & -0.05 & -0.02 & 0 \\ -0.01 & 0.015 & 0.003 & 0 & 0.07 & 0 \\ 0 & 0.05 & 0 & 0.1 & 0.02 & 0.02 \\ 0 & 0.02 & -0.07 & 0.02 & 0.05 & 0 \\ 0.03 & 0 & 0 & -0.02 & 0 & 0.1 \end{bmatrix}$$

$$\bar{\mathbf{G}}^m_1 = \bar{\mathbf{G}}^m_3 = \mathbf{0}, \bar{\mathbf{G}}^m_2 = diag\{0.05, 0.026, 0.01, 0.03, 0.01, 0.01\}$$

$$\bar{\mathbf{G}}^r_1 = \begin{bmatrix} 0 & 0 & 0 & 0 & 0 & 0 \\ 0 & 0 & 0 & 0 & 0 & 0 \\ 0 & 0 & 0.2 & 0.09 & 0 & 0 \\ 0 & 0 & 0.09 & 0.35 & 0 & 0 \\ 0 & 0 & 0 & 0 & 0.17 & 0 \\ 0 & 0 & 0 & 0 & 0 & 0 \end{bmatrix}, \bar{\mathbf{G}}^r_2 = \bar{\mathbf{G}}^r_3 = \bar{\mathbf{G}}^r_1$$

$$\mathbf{d}_1 = \mathbf{d}_2 = \mathbf{d}_3 = 0.05\sin(0.5t)[1\ 1\ 0.5\ 0.5\ 0.3\ 0.3]^T.$$

The hydrodynamic damping, restoring, and mooring terms are used for simulation, but are considered to be unknown in the control design. To emulate the changes in mass matrix changes during switching, let us consider

$$\bar{\mathbf{M}}_{\sigma(t)} = \begin{cases} \mathbf{M}_{\text{in}}, & 0 \le t < 45 \\ 0.9\mathbf{M}_{\text{in}}, & 45 \le t < 110 \\ 0.8\mathbf{M}_{\text{in}}, & 110 \le t < 180 \\ 0.7\mathbf{M}_{\text{in}}, & t \ge 180 \end{cases}$$

$$\mathbf{M}_{\text{in}} = \begin{bmatrix} 1 & 0 & 0 & -0.05 & 0 & 0 \\ 0 & 2 & -0.5 & 0 & -0.05 & -0.5 \\ 0 & -0.5 & 1 & 0 & 0 & -0.05 \\ -0.05 & 0 & 0 & 0.1 & 0 & 0 \\ 0 & -0.05 & 0 & 0 & 0.1 & 0 \\ 0 & -0.5 & -0.05 & 0 & 0 & 0.2 \end{bmatrix}.$$

B. Results

It is standard in literature (cf., [2]–[4], [12]–[16], [20], and [29]) to organize the system dynamics in way to group the actuated and nonactuated states together as in (3). Let

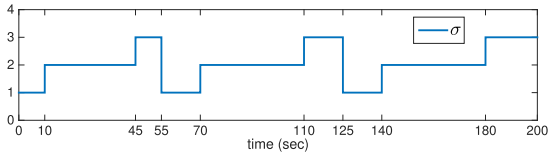

Fig. 2. Switching signal.

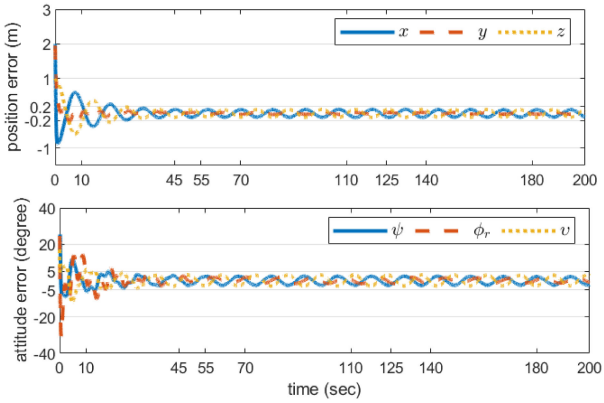

Fig. 3. Tracking performance of the proposed controller with external disturbance ($\mathbf{d}_\sigma \neq \mathbf{0}$).

$\check{\mathbf{E}}_\sigma = \{\check{E}_{i\sigma}\}$ and $\check{\mathbf{d}}_\sigma = \{\check{d}_{i\sigma}\}$, $i = 1, \ldots, 6$. Then, by rearranging $\mathbf{q} = [x, y, \psi, z, \phi_r, \upsilon]^T$, one can represent (27) in the form of (3) with $\mathbf{E}_\sigma = [\check{E}_{1\sigma}, \check{E}_{2\sigma}, \check{E}_{6\sigma}, \check{E}_{3\sigma}, \check{E}_{4\sigma}, \check{E}_{5\sigma}]^T$, $\mathbf{d}_\sigma = [\check{d}_{1\sigma}, \check{d}_{2\sigma}, \check{d}_{6\sigma}, \check{d}_{3\sigma}, \check{d}_{4\sigma}, \check{d}_{5\sigma}]^T$, $\boldsymbol{\tau}_\sigma = [\tau_{x\sigma}, \tau_{y\sigma}, \tau_{\psi\sigma}]$, and an appropriate $\mathbf{M}_\sigma(\mathbf{q})$ (not shown for lack of space). Denoting $\mathbf{q_a} = \{x, y, \psi\}$ and $\mathbf{q_u} = \{z, \phi_r, \upsilon\}$, the crane vessel dynamics can be represented as in (8) with $n = 6$ and $m = 3$, where the *Properties 1 and 2* are satisfied [32, Sec. 7.5]. Therefore, one can verify that the upper bound structures (15), (16), and (21) hold. It is possible to verify that the mass matrix considered herein (cf., the general mass matrix structure in [32, Sec. 7.5, eq. (7.197]) satisfies Assumption 3.

The desired trajectories are $\mathbf{q}^d = \dot{\mathbf{q}}^d = \ddot{\mathbf{q}}^d = \mathbf{0}$. The nominal mass matrix is taken based on $\hat{\bar{\mathbf{M}}}_\sigma = 0.8\mathbf{M}_{\text{in}}\ \forall \sigma \in \{1, 2, 3\}$ to compute $\hat{\mathbf{b}}_\sigma$ in (12a). It can be verified that (13) holds with $\alpha = 0.5$. Therefore, the actual mass matrix is also uncertain for control design. Other control parameters are designed as follows: $\boldsymbol{\Lambda}_1 = 12\mathbf{I}, \boldsymbol{\Lambda}_2 = 15\mathbf{I}, \boldsymbol{\Lambda}_3 = 10\mathbf{I}, \boldsymbol{\Gamma}_\mathbf{a} = \boldsymbol{\Gamma}_\mathbf{u} = 10\mathbf{I}, \boldsymbol{\Upsilon}_\mathbf{a} = \boldsymbol{\Upsilon}_\mathbf{u} = 2\mathbf{I}, \mathbf{H}_1 = 10\mathbf{I}, \mathbf{H}_2 = 15\mathbf{I}, \mathbf{H}_3 = 20\mathbf{I}, \mathbf{Q}_\sigma = \mathbf{I}, \epsilon = 0.1, \varphi = 1.1, \zeta_{i\sigma} = 1, \delta_{0\sigma} = 0.3, \delta_{1\sigma} = 0.1, \delta_{2\sigma} = 1, \overline{\varsigma}_\sigma = 0.2, \nu_\sigma = 0.1, \overline{\nu}_\sigma = 0.1$, $\underline{\alpha} = 5, \beta_\sigma = 11.5$, and $\hat{\theta}_{i\sigma}(0) = \eta_\sigma(0) = \gamma_\sigma(0) = 0.5\ \forall \sigma$ and $i = 0, 1, 2$, satisfying the design conditions listed in (23). The initial condition is selected as $\mathbf{q}(0) = [2\ 2\ 1\ 0.5\ 0.3\ 0.3]^T$. The simulated operation as in Fig. 2 yields desired ADT $\vartheta = 25$ s (eight switchings in 200 s operation); and the gain selections yield $\kappa_M = 2.6, \kappa_m = 1.1 \times 10^{-3}$ leading to $\ln \mu/\varrho = 20.18$, and thus, satisfying the switching law of $\vartheta > \ln \mu/\varrho$ from (25). The switching law $\sigma(t)$ is designed as in Fig. 2, which is in accordance with offshore operation, where mooring phases take longer time of completion.

The performance of the proposed controller in the presence of the external disturbances $\mathbf{d}_\sigma$ is depicted in Fig. 3: the corresponding gains in Fig. 4 reveal that, for an active (resp., inactive) mode, the gains $\hat{\theta}_{ip}$ and η_p (resp. $\gamma_{\overline{p}}$) are updated, while γ_p (resp., $\hat{\theta}_{i\overline{p}}, \eta_{\overline{p}}$) remains constant for the switch-ON (resp., switch-OFF) period. To show that the residual tracking errors are affected by disturbance terms, we report

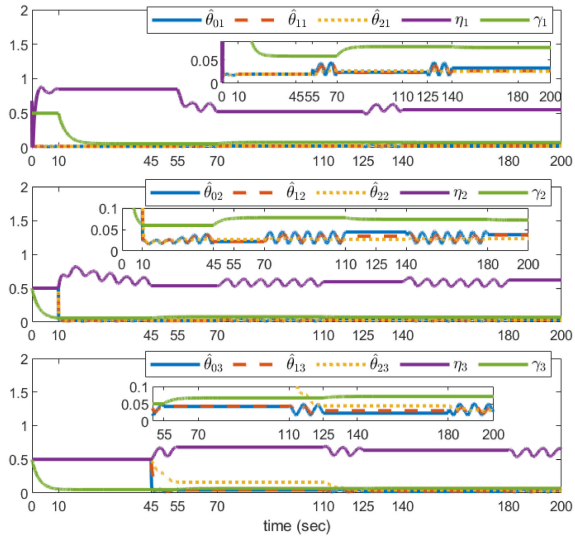

Fig. 4. Evolution of various gains with $\mathbf{d}_\sigma \neq \mathbf{0}$.

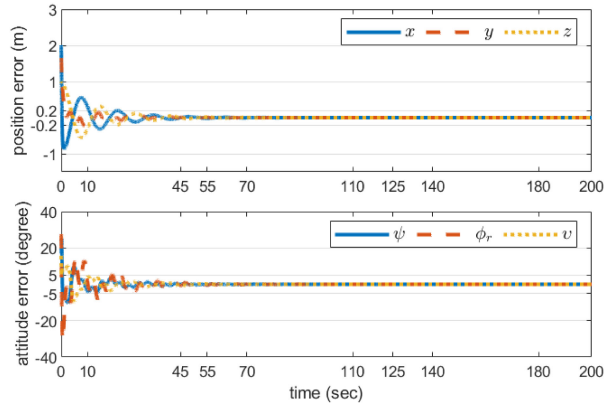

Fig. 5. Tracking performance of the proposed controller without external disturbance ($\mathbf{d}_\sigma = \mathbf{0}$).

in Fig. 5, the tracking errors when the external disturbances $\mathbf{d}_\sigma$ are removed.

V. Conclusion

This note proposed an adaptive control design for a class of underactuated EL systems under various sources of uncertainties and switched dynamics due to changeable operating regimes. We established stability and robustness of the closed-loop system, and the performance of the proposed design was validated using an underactuated offshore crane vessel.

Appendix

Proof of Theorem 1: It can be verified from the adaptive laws (23a)–(23c) and the initial gain conditions (23f) that

$$\hat{\theta}_{i\sigma}(t) \geq 0,\ \eta_\sigma(t) \geq \underline{\eta}_\sigma > 0 \text{ and } \gamma_\sigma(t) \geq \underline{\gamma}_\sigma > 0\ \forall t \geq t_0. \quad (28)$$

The closed-loop stability is analyzed using the Lyapunov candidate

$$V = \frac{1}{2}\left\{\mathbf{r}^T\mathbf{r} + \mathbf{x}^T\mathbf{P}_p\mathbf{x} + \sum_{s=1}^{N}\sum_{i=0}^{2}(\hat{\theta}_{is} - \bar{\theta}^*_{is})^2 + \eta_s^2 + \frac{2\gamma_s}{\underline{\gamma}}\right\} \tag{29}$$

where $\underline{\gamma} = \min_{p\in\Omega}\{\underline{\gamma}_p\}$. At the switching instant $t_{l+1},\ l \in \mathbb{N}^+$, let the active mode be $\sigma(t^-_{l+1})$ when $t \in [t_l \quad t_{l+1})$ and $\sigma(t_{l+1})$ when $t \in [t_{l+1} \quad t_{l+2})$. The continuity of $\mathbf{r}$ and $\mathbf{x}$ in (9) and (20) and of $\hat{\theta}_{i\sigma}$, η_σ, and γ_σ in (23), give the following equalities before and after switching $\mathbf{r}(t^-_{l+1}) = \mathbf{r}(t_{l+1}), \mathbf{x}(t^-_{l+1}) = \mathbf{x}(t_{l+1}), (\hat{\theta}_{is}(t^-_{l+1}) - \theta^*_{is}) = (\hat{\theta}_{is}(t_{l+1}) - \theta^*_{is}),\ \eta_s(t^-_{l+1}) = \eta_s(t_{l+1}),$ and $\gamma_s(t^-_{l+1}) = \gamma_s(t_{l+1})$. Furthermore, the upper and lower bounds $\mathbf{x}^T(t)\mathbf{P}_{\sigma(t)}\mathbf{x}(t) \le \kappa_M\mathbf{x}^T(t)\mathbf{x}(t)$ and $\mathbf{x}^T(t)\mathbf{P}_{\sigma(t)}\mathbf{x}(t) \ge \kappa_m\mathbf{x}^T(t)\mathbf{x}(t)$ give

$$\begin{aligned} V(t_{l+1}) - V(t^-_{l+1}) &= \frac{1}{2}\mathbf{x}^T(t_{l+1})(\mathbf{P}_{\sigma(t_{l+1})} - \mathbf{P}_{\sigma(t^-_{l+1})})\mathbf{x}(t_{l+1}) \\ &\le \frac{\kappa_M - \kappa_m}{2\kappa_m}\mathbf{x}^T(t_{l+1})\mathbf{P}_{\sigma(t^-_{l+1})}\mathbf{x}(t_{l+1}) \le \frac{\kappa_M - \kappa_m}{\kappa_m}V(t^-_{l+1}) \\ &\Rightarrow V(t_{l+1}) \le \mu V(t^-_{l+1}) \end{aligned} \tag{30}$$

with $\mu = \kappa_M/\kappa_m \ge 1$. Let us now consider a region such that $\varphi\frac{||\mathbf{r}||^2}{\sqrt{||\mathbf{r}||^2+\epsilon}} \ge ||\mathbf{r}| \Rightarrow ||\mathbf{r}|| \ge \sqrt{\frac{\epsilon}{\varphi^2-1}} \triangleq \bar{\epsilon}$, with a user defined $\varphi > 1$. We proceed with studying the behavior of $V(t)$ between two consecutive switching instants, i.e., when $t \in [t_l \quad t_{l+1})$, for the two case: 1) $||\mathbf{r}|| \ge \bar{\epsilon}$ and 2) $||\mathbf{r}|| < \bar{\epsilon}$. Let us denote the active mode $p = \sigma(t^-_{l+1})$ only as p for convenience, and any inactive mode as $\overline{p}$.

Case (1): $||\mathbf{r}|| \ge \bar{\epsilon}$. Using (12b), (16), and (22), (11) yields

$$\mathbf{r}^T\dot{\mathbf{r}} \le -\mathbf{r}^T\mathbf{\Lambda}_p\mathbf{r} - \sum_{i=0}^{2}\{(\hat{\theta}_{ip} - \bar{\theta}^*_{ip})||\boldsymbol{\xi}||^i + \eta_p + \gamma_p\}||\mathbf{r}|| \tag{31}$$

$$\frac{1}{2}\frac{\mathrm{d}}{\mathrm{d}t}\mathbf{x}^T\mathbf{P}_p\mathbf{x} \le -\frac{1}{2}\mathbf{x}^T\mathbf{Q}_p\mathbf{x} + \varpi_p\overline{\alpha}||\mathbf{x}|| + ||\overline{\overline{\phi}}_p||||\mathbf{P}_p\mathbf{B}||||\mathbf{x}||. \tag{32}$$

Let us substitute (21) into (32)

$$\begin{aligned} \frac{1}{2}\frac{\mathrm{d}}{\mathrm{d}t}\mathbf{x}^T\mathbf{P}_p\mathbf{x} \le -\frac{1}{2}\mathbf{x}^T\mathbf{Q}_p\mathbf{x} + \sum_{i=0}^{2}\{\bar{\theta}^*_{ip}||\boldsymbol{\xi}||^i||\mathbf{x}|| \\ + ((\varphi\overline{\alpha})/(1-\alpha))(\hat{\theta}_{ip}||\boldsymbol{\xi}||^i + \eta_p + \gamma_p)||\mathbf{x}||\}. \end{aligned} \tag{33}$$

The adaptive laws (23a) and (23b) yield, for $i = 0, 1, 2$

$$\begin{aligned} (\hat{\theta}_{ip} - \bar{\theta}^*_{ip})\dot{\hat{\theta}}_i &= \hat{\theta}_{ip}(||\mathbf{r}|| + ||\mathbf{x}||)||\boldsymbol{\xi}||^i - c_{ip}\hat{\theta}^2_{ip}||\mathbf{x}||||\boldsymbol{\xi}||^i \\ &\quad - \bar{\theta}^*_{ip}(||\mathbf{r}|| + ||\mathbf{x}||)||\boldsymbol{\xi}||^i + c_{ip}\hat{\theta}_{ip}\bar{\theta}^*_{ip}||\mathbf{x}||||\boldsymbol{\xi}||^i \end{aligned} \tag{34}$$

$$\begin{aligned} \eta_p\dot{\eta}_p &= \eta_p(||\mathbf{r}|| + ||\mathbf{x}||) + \eta_p\delta_{0p}\nu_p \\ &\quad - \eta_p^2\{\delta_{0p} + \delta_{1p}(||\boldsymbol{\xi}||^5 - ||\boldsymbol{\xi}||^4) + \delta_{2p}||\mathbf{x}||)\} \end{aligned} \tag{35}$$

where $c_{ip} \triangleq \zeta_{ip}\beta_p$. One can verify that, by design, $c_{ip} \in \mathbb{R}^+$ as $\beta_p, \zeta_{ip} \in \mathbb{R}^+$. Similarly, (23c) leads to for $\overline{p} \in \Omega\backslash\{p\}$

$$\frac{\dot{\gamma}_{\overline{p}}}{\underline{\gamma}} = \frac{-(\overline{\varsigma}_{\overline{p}} + \frac{\varrho_{\overline{p}}}{2}(\sum_{i=0}^{2}\hat{\theta}^2_{i\overline{p}} + \eta^2_{\overline{p}}))\gamma_{\overline{p}} + \overline{\varsigma}_{\overline{p}}\overline{\nu}_{\overline{p}}}{\underline{\gamma}}. \tag{36}$$

Applying (28) to the second term of (36) yields

$$\frac{\dot{\gamma}_{\overline{p}}}{\underline{\gamma}} \le -\overline{\varsigma}_{\overline{p}}\frac{\gamma_{\overline{p}}}{\underline{\gamma}} - \frac{\varrho_{\overline{p}}}{2}\left(\sum_{i=0}^{2}\hat{\theta}^2_{i\overline{p}} + \eta^2_{\overline{p}}\right) + \frac{\overline{\varsigma}_{\overline{p}}\overline{\nu}_{\overline{p}}}{\underline{\gamma}}. \tag{37}$$

Therefore

$$\begin{aligned} &\frac{\mathrm{d}}{\mathrm{d}t}\left(\sum_{s=1}^{N}\sum_{i=0}^{2}\frac{(\hat{\theta}_{is} - \bar{\theta}^*_{is})^2}{2} + \frac{\eta_s^2}{2} + \frac{\gamma_s}{\underline{\gamma}}\right) \\ &\le \sum_{i=0,p=\sigma(t^-_{l+1})}^{2}\{\hat{\theta}_{ip}(||\mathbf{r}|| + ||\mathbf{x}||)||\boldsymbol{\xi}||^i - c_{ip}\hat{\theta}^2_{ip}||\mathbf{x}||||\boldsymbol{\xi}||^i \\ &- \bar{\theta}^*_{ip}(||\mathbf{r}|| + ||\mathbf{x}||)||\boldsymbol{\xi}||^i + c_{ip}\hat{\theta}_i\bar{\theta}^*_i||\mathbf{x}||||\boldsymbol{\xi}||^i + \eta_p(||\mathbf{r}|| + ||\mathbf{x}||) \\ &- \eta_p^2\left(\delta_{0p} + \delta_{1p}(||\boldsymbol{\xi}||^5 - ||\boldsymbol{\xi}||^4) + \delta_{2p}||\mathbf{x}||\right) + \eta_p\delta_{0p}\nu_p\} \\ &- \sum_{\overline{p}\in\Omega\backslash\{p\}}\left\{\overline{\varsigma}_{\overline{p}}\frac{\gamma_{\overline{p}}}{\underline{\gamma}} + \frac{\varrho_{\overline{p}}}{2}\left(\sum_{i=0}^{2}\hat{\theta}^2_{i\overline{p}} + \eta^2_{\overline{p}}\right) - \frac{\overline{\varsigma}_{\overline{p}}\overline{\nu}_{\overline{p}}}{\underline{\gamma}}\right\}. \end{aligned} \tag{38}$$

Let us now use (31), (33), and (38) into the time derivative of (29), resulting in

$$\begin{aligned} \dot{V} \le\ &-\varrho_{mp}(||\mathbf{r}||^2 + ||\mathbf{x}||^2) + \eta_p\delta_{0p}\nu_p + c_p(\eta_p + \gamma_p)||\mathbf{x}|| \\ &- \eta_p^2\left(\delta_{0p} + \delta_{1p}(||\boldsymbol{\xi}||^5 - ||\boldsymbol{\xi}||^4) + \delta_{2p}||\mathbf{x}||\right) \\ &+ \sum_{i=0}^{2}\left(c_p\hat{\theta}_{ip} - c_{ip}\hat{\theta}^2_{ip} + c_{ip}\hat{\theta}_{ip}\bar{\theta}^*_{ip}\right)||\boldsymbol{\xi}||^i||\mathbf{x}|| \\ &- \sum_{\overline{p}\in\Omega\backslash\{p\}}\left\{\overline{\varsigma}_{\overline{p}}\frac{\gamma_{\overline{p}}}{\underline{\gamma}} + \frac{\varrho_{\overline{p}}}{2}\left(\sum_{i=0}^{2}\hat{\theta}^2_{i\overline{p}} + \eta^2_{\overline{p}}\right) - \frac{\overline{\varsigma}_{\overline{p}}\overline{\nu}_{\overline{p}}}{\underline{\gamma}}\right\} \end{aligned} \tag{39}$$

where $\varrho_{mp} \triangleq \min\{\lambda_{\min}(\mathbf{\Lambda}_p),\ (1/2)\lambda_{\min}(\mathbf{Q}_p)\}$ and $c \triangleq 1 + \frac{\varphi\overline{\alpha}}{1-\alpha}$. Since $\hat{\theta}_i(t) \ge 0$, the following inequality holds from (29):

$$V \le \varrho_{Mp}(||\mathbf{r}||^2 + ||\mathbf{x}||^2) + \sum_{s=1}^{N}\sum_{i=0}^{2}\frac{(\hat{\theta}^2_{is} + \bar{\theta}^{*2}_{is})}{2} + \frac{\eta_s^2}{2} + \frac{\gamma_s}{\underline{\gamma}} \tag{40}$$

where $\varrho_{Mp} \triangleq \max\{(1/2),\ (1/2)\lambda_{\max}(\mathbf{P}_p)\}$. Using the definition of ϱ_p from (24), the design conditions (23d) and the upper bound (40), the inequality (39) is further simplified to

$$\begin{aligned} \dot{V} \le\ &-\varrho V + \sum_{s=1}^{N}\sum_{i=0}^{2}\frac{\varrho_s\bar{\theta}^{*2}_{is}}{2} + \sum_{\overline{p}\in\Omega\backslash\{p\}}\frac{\overline{\varsigma}_{\overline{p}}\overline{\nu}_{\overline{p}}}{\underline{\gamma}} \\ &+ \sum_{i=0,p=\sigma(t^-_{l+1})}^{2}\{\eta_p\delta_{0p}\nu_p + c(\eta_p + \gamma_p)||\mathbf{x}|| + \frac{\varrho_p\gamma_p}{\underline{\gamma}} \\ &- \eta_p^2\left(\bar{\delta}_{0p} + \delta_{1p}(||\boldsymbol{\xi}||^5 - ||\boldsymbol{\xi}||^4) + \delta_{2p}||\mathbf{x}||\right) \\ &+ (c\hat{\theta}_{ip} - c_{ip}\hat{\theta}^2_{ip} + c_{ip}\hat{\theta}_{ip}\bar{\theta}^*_{ip})||\boldsymbol{\xi}||^i||\mathbf{x}|| + (\varrho_p\hat{\theta}^2_{ip})/2\} \end{aligned} \tag{41}$$

where $\varrho \triangleq \min_{p\in\Omega}\{\varrho_p\}$ and $\bar{\delta}_{0p} \triangleq (\delta_{0p} - \frac{\varrho_p}{2}) > 0$ [cf., (23d)]. For ease of analysis, the positive constants c_{ip} and δ_{2p} are split as

$$c_{ip} = \sum_{j=1}^{3}c_{ipj},\ \delta_{2p} = \sum_{k=1}^{2}\delta_{2pk},\ c_{ipj}, \delta_{2pk} > 0\ \forall i, j, k \tag{42}$$

resulting in

$$\begin{aligned} &-c_{ip}\hat{\theta}^2_{ip} + c\hat{\theta}_{ip} + c_{ip}\hat{\theta}_{ip}\bar{\theta}^*_{ip} \\ &= -c_{ip1}\hat{\theta}^2_{ip} - c_{ip2}\{(\hat{\theta}_{ip} - (c/(2c_{ip2})))^2 - (c^2/(4c^2_{ip2}))\} \\ &- c_{ip3}\{(\hat{\theta}_{ip} - ((c_{ip}\bar{\theta}^*_{ip})/(2c_{ip3})))^2 - ((c_{ip}\bar{\theta}^*_{ip})^2/(4c^2_{ip3}))\} \\ &\le -c_{ip1}\hat{\theta}^2_{ip} + c^2/(4c_{ip2}) + (c_{ip}\bar{\theta}^*_{ip})^2/(4c_{ip3}) \end{aligned} \tag{43}$$

and, along similar lines as (43)

$$-\underline{\eta}_p^2(\bar{\delta}_{0p}+\delta_{2p}||\mathbf{x}||)+\eta_p\delta_{0p}\nu_p+c\eta_p||\mathbf{x}||$$
$$\leq -\delta_{2p1}\underline{\eta}_p^2||\mathbf{x}||+\left(c^2/4\delta_{2p2}\right)||\mathbf{x}||+((\delta_{0p}\nu_p)^2/4\bar{\delta}_{0p}). \quad (44)$$

Using the inequalities $\eta_p \geq \underline{\eta}_p > 0$ and $||\boldsymbol{\xi}|| \geq ||\mathbf{x}||$ and (43) and (44), the time derivative (41) becomes

$$\dot{V} \leq -\varrho V+\sum_{s=1}^{N}\sum_{i=0}^{2}\frac{\varrho_s\bar{\theta}_{is}^{*2}}{2}+\sum_{\overline{p}\in\Omega\setminus\{p\}}\frac{\overline{\varsigma}_{\overline{p}}\overline{\nu}_{\overline{p}}}{\underline{\gamma}}$$
$$+\sum_{i=0,p=\sigma(t_{l+1}^-)}^{2}\left\{\left(\frac{c^2}{4c_{ip2}}+\frac{(c_{ip}\bar{\theta}_{ip}^*)^2}{4c_{ip3}}\right)\right.$$
$$||\boldsymbol{\xi}||^{i+1}-c_{ip1}\hat{\theta}_{ip}^2||\mathbf{x}||^{i+1}$$
$$+\left(\varrho_p\hat{\theta}_{ip}^2\right)/2-\underline{\eta}_p^2\delta_{1p}\left(||\boldsymbol{\xi}||^5-||\boldsymbol{\xi}||^4\right)+(c^2||\mathbf{x}||)/(4\delta_{2p2})$$
$$\left.+(\delta_{0p}\nu_p)^2/(4\bar{\delta}_{0p})+(\varrho_p\gamma_p)/\underline{\gamma}\right\}$$
$$=-\varrho V-\sum_{i=0,p=\sigma(t_{l+1}^-)}^{2}\hat{\theta}_{ip}^2\left(c_{ip1}||\mathbf{x}||^{i+1}-\frac{\varrho_p}{2}\right)+f_p(||\boldsymbol{\xi}||)$$

where $f_p(||\boldsymbol{\xi}||) \triangleq -\underline{\eta}_p^2\delta_{1p}||\boldsymbol{\xi}||^5+\omega_{4p}||\boldsymbol{\xi}||^4+\omega_{3p}||\boldsymbol{\xi}||^3$
$$+\omega_{2p}||\boldsymbol{\xi}||^2+\omega_{1p}||\boldsymbol{\xi}||+\omega_{0p}$$
$$\omega_{3p} \triangleq c^2/(4c_{2p2})+\left(\left(c_{2p}\bar{\theta}_{2p}^*\right)^2/(4c_{2p3})\right), \omega_{4p} \triangleq \underline{\eta}_p^2\delta_{1p}$$
$$\omega_{2p} \triangleq \frac{c^2}{4c_{1p2}}+\frac{\left(c_{1p}\bar{\theta}_{1p}^*\right)^2}{4c_{1p3}}, \omega_{1p} \triangleq \frac{c^2}{4c_{0p2}}+\frac{\left(c_{0p}\bar{\theta}_{0p}^*\right)^2}{4c_{0p3}}+\frac{c^2}{4\delta_{2p2}}$$
$$\omega_{0p} \triangleq \frac{(\delta_{0p}\nu_p)^2}{4\bar{\delta}_{0p}}+\frac{\varrho_p\bar{\gamma}_p}{\underline{\gamma}}+\sum_{p=1}^{N}\sum_{i=0}^{2}\frac{\varrho_p\bar{\theta}_{ip}^{*2}}{2}+\sum_{\overline{p}\in\Omega\setminus\{p\}}\frac{\overline{\varsigma}_{\overline{p}}\overline{\nu}_{\overline{p}}}{\underline{\gamma}} \quad (45)$$

where $\bar{\gamma}_p \geq \gamma_p(t)$ [from the adaptive laws for γ_p in (23)]. Applications of Descartes' rule of sign change and Bolzano's Theorem yield polynomial f_p has exactly one positive real root and let $\iota_p \in \mathbb{R}^+$ be that positive real root. The coefficient of the highest degree of f_p is negative as $\underline{\eta}_p^2\delta_{1p} \in \mathbb{R}^+$. Therefore, $f_p(||\boldsymbol{\xi}||) \leq 0$ when $||\boldsymbol{\xi}|| \geq \iota_p$. Furthermore, define $\iota_{0p} \triangleq (\varrho_p/2c_{0p1}), \iota_{1p} \triangleq \sqrt{\varrho_p/2c_{1p1}}$, and $\iota_{2p} \triangleq (\varrho_p/2c_{2p1})^{1/3}$. As $V \geq \frac{\lambda_{\min}(\mathbf{P}_p)}{2}||\mathbf{x}||^2$ [cf., (29)], we have $\dot{V} \leq -\varrho V$ for Case (1) from (45) when, for $i = 0, 1, 2$,

$$\min\{||\mathbf{x}||, ||\boldsymbol{\xi}||\} \geq \max_{p\in\Omega}\{\iota_p,\ \iota_{ip}\} \Rightarrow ||\mathbf{x}|| \geq \max_{p\in\Omega}\{\iota_p,\ \iota_{ip}\}$$
$$\Rightarrow V \geq (1/2)\max_{p\in\Omega}\{\lambda_{\min}(\mathbf{P}_p)\iota_p^2,\ \lambda_{\min}(\mathbf{P}_p)\iota_{ip}^2\} \triangleq \mathcal{B}_1. \quad (46)$$

Case (2): $||\mathbf{r}|| < \bar{\epsilon}$. Using (12b), (16), and (22), (11) yields

$$\mathbf{r}^T\dot{\mathbf{r}} \leq -\mathbf{r}^T\boldsymbol{\Lambda}_p\mathbf{r}-(1-\alpha)\varpi_p\frac{||\mathbf{r}||^2}{\sqrt{||\mathbf{r}||^2+\epsilon}}+\sum_{i=0}^{2}\theta_{ip}^*||\boldsymbol{\xi}||^i||\mathbf{r}||$$
$$\leq -\mathbf{r}^T\boldsymbol{\Lambda}_p\mathbf{r}+\sum_{i=0}^{2}\bar{\theta}_{ip}^*||\boldsymbol{\xi}||^i||\mathbf{r}||. \quad (47)$$

The following simplification is made for $i = 0, 1, 2$:

$$\bar{\epsilon}\hat{\theta}_{ip}||\boldsymbol{\xi}||^i = \hat{\theta}_{ip}^2-\{(\hat{\theta}_{ip}-(\bar{\epsilon}||\boldsymbol{\xi}||^i)/2)^2-(\bar{\epsilon}^2||\boldsymbol{\xi}||^{(2i)})/4\}$$
$$\leq \hat{\theta}_{ip}^2+(\bar{\epsilon}^2||\boldsymbol{\xi}||^{(2i)})/4. \quad (48)$$

Using (47) and (48) and along similar lines as Case (1), we arrive at the following inequality for Case (2):

$$\dot{V} \leq -\varrho V-\sum_{i=0,p=\sigma(t_{l+1}^-)}^{2}\hat{\theta}_{ip}^2(c_{ip1}||\mathbf{x}||^{i+1}-\frac{\varrho_p}{2}-1)+\bar{f}_p$$
$$\text{with}\quad \bar{f}_p(||\boldsymbol{\xi}||) \triangleq -\underline{\eta}_p^2\delta_{1p}||\boldsymbol{\xi}||^5+\omega'_{4p}||\boldsymbol{\xi}||^4+\omega_{3p}||\boldsymbol{\xi}||^3$$
$$+\omega'_{2p}||\boldsymbol{\xi}||^2+\omega_{1p}||\boldsymbol{\xi}||+\omega'_{0p}$$
$$\omega'_{4p} \triangleq \omega_4+(\bar{\epsilon}^2/4), \omega'_2 \triangleq \omega_2+(\bar{\epsilon}^2/4)$$
$$\omega'_{0p} \triangleq \frac{\bar{\epsilon}^2}{4}+\frac{(\delta_{0p}\nu_p)^2}{4\bar{\delta}_{0p}}+\frac{\varrho_p\bar{\gamma}_p}{\underline{\gamma}}+\sum_{p=1}^{N}\sum_{i=0}^{2}\frac{\varrho_p\bar{\theta}_{ip}^{*2}}{2}+\sum_{\overline{p}\in\Omega\setminus\{p\}}\frac{\overline{\varsigma}_{\overline{p}}\overline{\nu}_{\overline{p}}}{\underline{\gamma}}. \quad (49)$$

Therefore, for Case (2), $\dot{V} \leq -\varrho V$ is guaranteed when

$$V \geq (1/2)\max_{p\in\Omega}\{\lambda_{\min}(\mathbf{P}_p){\iota'_p}^2,\ \lambda_{\min}(\mathbf{P}_p){\iota'_{ip}}^2\} \triangleq \mathcal{B}_2 \quad (50)$$

where ι'_p is the sole positive real root of $\bar{f}_p$ and $\iota'_{ip} \triangleq (\frac{\varrho_p}{2c_{ip1}}+\frac{1}{c_{ip1}})^{\frac{1}{i+1}}$, $i = 0, 1, 2$. Hence, investigating (46) and (50), it can be concluded that $\dot{V} \leq -\varrho V$ is guaranteed when

$$V \geq \max\{\mathcal{B}_1,\ \mathcal{B}_2\} \triangleq \mathcal{B}.$$

In light of this, further analysis is needed to observe the behavior of $V(t)$ for the following two possible scenarios:

1) when $V(t) \geq \mathcal{B}$, we have $\dot{V}(t) \leq -\varrho V(t)$ implying exponential decrease of $V(t)$;
2) when $V(t) < \mathcal{B}$, no exponential decrease can be derived.

Scenario (1): There exists a time, call it T_1, when $V(t)$ enters into the bound $\mathcal{B}$ and $N_\sigma(t)$ denotes the number of all switching intervals for $t \in [t_0\ \ t_0+T_1)$. From Definition 1, for $t \in [t_0\ \ t_0+T_1)$, using (30) and $N_\sigma(t_0, t)$, we have

$$V(t) \leq \exp\left(-\varrho(t-t_{N_\sigma(t)-1})\right)V(t_{N_\sigma(t)-1})$$
$$\leq \mu\exp\left(-\varrho(t-t_{N_\sigma(t)-1})\right)\mu\exp\left(-\varrho(t_{N_\sigma(t)-1}-t_{N_\sigma(t)-2})\right)$$
$$\cdots\mu\exp\left(-\varrho(t_1-t_0)\right)V(t_0)$$
$$=b\left(\exp\left(-\varrho+(\ln\mu/\vartheta)\right)(t-t_0)\right)V(t_0) \quad (51)$$

where $b \triangleq \exp(N_0\ln\mu)$ is a constant. Substituting the ADT condition $\vartheta > \ln\mu/\varrho$ into (51) yields $V(t) < bV(t_0)$ for $t \in [t_0\ t_0+T_1)$. Moreover, as $V(t_0+T_1) < \mathcal{B}$, one has $V(t_{N_\sigma(t)+1}) < \mu\mathcal{B}$ from (30) at the next switching instant $t_{N_\sigma(t)+1}$ after t_0+T_1, implying that $V(t)$ may be larger than $\mathcal{B}$ from the instant $t_{N_\sigma(t)+1}$. Hence, we assume $V(t) \geq \mathcal{B}$ for $t \in [t_{N_\sigma(t)+1}\ \ t_0+T_2)$, where T_2 denotes the time before the next switching. Let $\bar{N}_\sigma(t)$ represents the number of all switching intervals for $t \in [t_{N_\sigma(t)+1}\ t_0+T_2)$. Then, substituting $V(t_0)$ with $V(t_{N_\sigma(t)+1})$ into (51) and following the similar procedure for analysis as (51), we have $V(t) \leq bV(t_{N_\sigma(t)+1}) < b\mu\mathcal{B}$ for $t \in [t_{N_\sigma(t)+1}\ \ t_0+T_2)$. Since $V(t_0+T_2) < \mathcal{B}$, we have $V(t_{N_\sigma(t)+\bar{N}_\sigma(t)+2}) < \mu\mathcal{B}$ at the next switching instant $t_{N_\sigma(t)+\bar{N}_\sigma(t)+2}$ after t_0+T_2. Following similar lines of proof recursively implies $V(t) < b\mu\mathcal{B}$ for $t \in [t_0+T_1\ \infty)$ with (25).

Scenario (2): It can be easily verified that the same aforementioned argument also holds for Scenario (2).

From the analysis of Scenarios (1) and (2), it can be concluded that

$$V(t) \leq \max\{bV(t_0), b\mu\mathcal{B}\}\ \ \forall t \geq t_0. \quad (52)$$

The aforementioned conclusion implies $\mathbf{r}, \mathbf{e_u}, \dot{\mathbf{e}}_\mathbf{u}, \hat{\theta}_{i\sigma}, \eta_\sigma, \gamma_\sigma \in \mathcal{L}_\infty$ $\forall \sigma \in \Omega$. Furthermore, if (9) is rewritten as

$$\dot{\mathbf{e}}_\mathbf{a} = -\boldsymbol{\Upsilon}_\mathbf{a}^{-1}\boldsymbol{\Gamma}_\mathbf{a}\mathbf{e}_\mathbf{a} - \boldsymbol{\Upsilon}_\mathbf{a}^{-1}(\boldsymbol{\Upsilon}_\mathbf{u}\dot{\mathbf{e}}_\mathbf{u} + \boldsymbol{\Gamma}_\mathbf{u}\mathbf{e}_\mathbf{u}) + \boldsymbol{\Upsilon}_\mathbf{a}^{-1}\mathbf{r} \tag{53}$$

where $\boldsymbol{\Upsilon}_\mathbf{a}^{-1}$ exists being $\boldsymbol{\Upsilon}_\mathbf{a} > \mathbf{0}$, we have that $\mathbf{e_a}, \dot{\mathbf{e}}_\mathbf{a} \in \mathcal{L}_\infty$ (due to the fact that $\boldsymbol{\Upsilon}_\mathbf{a}^{-1}\boldsymbol{\Gamma}_\mathbf{a} > \mathbf{0}$ and $\mathbf{r}, \mathbf{e_u}, \dot{\mathbf{e}}_\mathbf{u} \in \mathcal{L}_\infty$). Furthermore, because $V \geq (1/2)||\mathbf{r}||^2$ from (29), and using (52) and the definition from [34, Sec. 4.8], an ultimate bound on the tracking error variable $\mathbf{r}$ is

$$\mathcal{B}_r = \sqrt{2b\mu\mathcal{B}}. \tag{54}$$

The condition (54) reveals that the ultimate bound is affected by the switching constant μ in (30) and by $\iota_p, \iota_{ip}, \iota_p, {}' \iota'_{ip}$, which are governed by the design parameters entering the polynomials $f_p(||\boldsymbol{\xi}||)$ and $\overline{f}_p(||\boldsymbol{\xi}||)$ in (45) and (49). For example, lower values of ϱ_σ in (24) [by tuning design parameters $\mathbf{K}_{1\sigma}$ and $\mathbf{K}_{2\sigma}$ via (19)] and higher values of δ_{2p} in (23b) help reducing $\mathcal{B}_r$.

Remark 7 (Multiple Lyapunov framework): Note that the Lyapunov function (29) depends on the active mode, known in literature as the multiple Lyapunov framework [27], and requires to study the behavior of the Lyapunov function at and in between switching instants [cf., (30), (45), (49), and (51)].

REFERENCES

[1] M. W. Spong, S. Hutchinson, and M. Vidyasagar, *Robot Modeling and Control*. Hoboken, NJ, USA: Wiley, 2005.

[2] J. Huang, S. Ri, T. Fukuda, and Y. Wang, "A disturbance observer based sliding mode control for a class of underactuated robotic system with mismatched uncertainties," *IEEE Trans. Autom. Control*, vol. 64, no. 6, pp. 2480–2487, Jun. 2019.

[3] R. Olfati-Saber, "Normal forms for underactuated mechanical systems with symmetry," *IEEE Trans. Autom. Control*, vol. 47, no. 2, pp. 305–308, Feb. 2002.

[4] B. Lu, Y. Fang, and N. Sun, "Continuous sliding mode control strategy for a class of nonlinear underactuated systems," *IEEE Trans. Autom. Control*, vol. 63, no. 10, pp. 3471–3478, Oct. 2018.

[5] A. H. Brodtkorb, S. A. Værnø, A. R. Teel, A. J. Sørensen, and R. Skjetne, "Hybrid controller concept for dynamic positioning of marine vessels with experimental results," *Automatica*, vol. 93, pp. 489–497, 2018.

[6] A. J. Sørensen, "A survey of dynamic positioning control systems," *Annu. Rev. Control*, vol. 35, no. 1, pp. 123–136, 2011.

[7] Z.-E. Lou and J. Zhao, "Immersion-and invariance-based adaptive stabilization of switched nonlinear systems," *Int. J. Robust Nonlinear Control*, vol. 28, no. 1, pp. 197–212, 2018.

[8] G. Lai, Z. Liu, Y. Zhang, C. P. Chen, and S. Xie, "Adaptive backstepping-based tracking control of a class of uncertain switched nonlinear systems," *Automatica*, vol. 91, pp. 301–310, 2018.

[9] M.-L. Chiang and L.-C. Fu, "Adaptive stabilization of a class of uncertain switched nonlinear systems with backstepping control," *Automatica*, vol. 50, no. 8, pp. 2128–2135, 2014.

[10] E. B. Kosmatopoulos and P. A. Ioannou, "A switching adaptive controller for feedback linearizable systems," *IEEE Trans. Autom. Control*, vol. 44, no. 4, pp. 742–750, Apr. 1999.

[11] E. B. Kosmatopoulos and P. A. Ioannou, "Robust switching adaptive control of multi-input nonlinear systems," *IEEE Trans. Autom. Control*, vol. 47, no. 4, pp. 610–624, Apr. 2002.

[12] R. Xu and Ü. Özgüner, "Sliding mode control of a class of underactuated systems," *Automatica*, vol. 44, no. 1, pp. 233–241, 2008.

[13] J. G. Romero, A. Donaire, R. Ortega, and P. Borja, "Global stabilisation of underactuated mechanical systems via PID passivity-based control," *Automatica*, vol. 96, pp. 178–185, 2018.

[14] B. Lu, Y. Fang, N. Sun, and X. Wang, "Antiswing control of offshore boom cranes with ship roll disturbances," *IEEE Trans. Control Syst. Technol.*, vol. 26, no. 2, pp. 740–747, Mar. 2018.

[15] B. Lu, Y. Fang, and N. Sun, "Modeling and nonlinear coordination control for an underactuated dual overhead crane system," *Automatica*, vol. 91, pp. 244–255, 2018.

[16] Y. Qian and Y. Fang, "Switching logic-based nonlinear feedback control of offshore ship-mounted tower cranes: A disturbance observer-based approach," *IEEE Trans. Autom. Sci. Eng.*, vol. 16, no. 3, pp. 1125–1136, Jul. 2019.

[17] P. A. Ioannou and J. Sun, *Robust Adaptive Control*. Upper Saddle River, NJ, USA: Prentice-Hall, 1996.

[18] Q. Sang and G. Tao, "Adaptive control of piecewise linear systems: The state tracking case," *IEEE Trans. Autom. Control*, vol. 57, no. 2, pp. 522–528, Feb. 2012.

[19] K. S. Narendra and A. M. Annaswamy, *Stable Adaptive Systems*. Chelmsford, MA, USA: Courier Corporation, 2012.

[20] M. W. Spong, "Partial feedback linearization of underactuated mechanical systems," in *Proc. IEEE/RSJ Int. Conf. Intell. Robots Syst.*, 1994, pp. 314–321.

[21] L. Long, Z. Wang, and J. Zhao, "Switched adaptive control of switched nonlinearly parameterized systems with unstable subsystems," *Automatica*, vol. 54, pp. 217–228, 2015.

[22] B. Zhao, B. Xian, Y. Zhang, and X. Zhang, "Nonlinear robust adaptive tracking control of a quadrotor UAV via immersion and invariance methodology," *IEEE Trans. Indus. Electron.*, vol. 62, no. 5, pp. 2891–2902, May 2015.

[23] T. Yang, N. Sun, H. Chen, and Y. Fang, "Neural network-based adaptive antiswing control of an underactuated ship-mounted crane with roll motions and input dead zones," *IEEE Trans. Neural Netw. Learn. Syst.*, vol. 31, no. 3, pp. 901–914, Mar. 2020.

[24] H. Ashrafiuon and R. S. Erwin, "Sliding mode control of underactuated multibody systems and its application to shape change control," *Int. J. Control*, vol. 81, no. 12, pp. 1849–1858, 2008.

[25] H. Ye, "Stabilization of uncertain feedforward nonlinear systems with application to underactuated systems," *IEEE Trans. Autom. Control*, vol. 64, no. 8, pp. 3484–3491, Aug. 2019.

[26] H. Ashrafiuon, S. Nersesov, and G. Clayton, "Trajectory tracking control of planar underactuated vehicles," *IEEE Trans. Autom. Control*, vol. 62, no. 4, pp. 1959–1965, Apr. 2017.

[27] J. P. Hespanha and A. S. Morse, "Stability of switched systems with average dwell-time," in *Proc. IEEE Conf. Decis. Control*, 1999, pp. 2655–2660.

[28] S. G. Nersesov, H. Ashrafiuon, and P. Ghorbanian, "On estimation of the domain of attraction for sliding mode control of underactuated nonlinear systems," *Int. J. Robust Nonlinear Control*, vol. 24, no. 5, pp. 811–824, 2014.

[29] A. Shkolnik and R. Tedrake, "High-dimensional underactuated motion planning via task space control," in *Proc. IEEE/RSJ Int. Conf. Intell. Robots Syst.*, 2008, pp. 3762–3768.

[30] Y. Shtessel, M. Taleb, and F. Plestan, "A novel adaptive-gain supertwisting sliding mode controller: Methodology and application," *Automatica*, vol. 48, no. 5, pp. 759–769, 2012.

[31] V. I. Utkin and A. S. Poznyak, "Adaptive sliding mode control with application to super-twist algorithm: Equivalent control method," *Automatica*, vol. 49, no. 1, pp. 39–47, 2013.

[32] T. I. Fossen, *Handbook of Marine Craft Hydrodynamics and Motion Control*. Hoboken, NJ, USA: Wiley, 2011.

[33] A. Grovlen and T. I. Fossen, "Nonlinear control of dynamic positioned ships using only position feedback: An observer backstepping approach," in *Proc. IEEE Conf. Decis. Control*, 1996, pp. 3388–3393.

[34] H. K. Khalil, *Nonlinear Systems*. Hoboken, NJ, USA: Prentice-Hall, 2002.